JOURNAL OF CHEMICAL PHYSICS VOLUME 119, NUMBER 1 1 JULY 2003

Two-pulse atomic coherent control spectroscopy of Eley–Rideal reactions: An application of an atom laser

Solvejg Jørgensen[a] and Ronnie Kosloff[b]
The Fritz Haber Research Center for Molecular Dynamics, Hebrew University, Jerusalem 91904, Israel

(Received 22 January 2003; accepted 31 March 2003)

A spectroscopic application of the atom laser is suggested. The spectroscopy termed 2PACC (two-pulse atomic coherent control) employs the coherent properties of matter waves from a two-pulse atom laser. These waves are employed to control a gas–surface chemical recombination reaction. The method is demonstrated for an Eley–Rideal reaction of a hydrogen or alkali atom-laser pulse where the surface target is an adsorbed hydrogen atom. The reaction yields either a hydrogen or alkali hydride molecule. The desorbed gas-phase molecular yield and its internal state is shown to be controlled by the time and phase delay between two atom-laser pulses. The calculation is based on solving the time-dependent Schrödinger equation in a diabatic framework. The probability of desorption which is the predicted 2PACC signal has been calculated as a function of the pulse parameters. © *2003 American Institute of Physics.* [DOI: 10.1063/1.1576383]

I. INTRODUCTION

Controlling the outcome of a chemical reaction has been the ultimate goal of chemistry. Coherent control, a new addition to the quest, is based on exploitation of quantum interferences of matter waves to build a constructive interference in the desired channel and a destructive interference in all other channels. To carry out such a task, the molecular matter wave has to exhibit a coherent property. To date, all experimental applications of coherent control have been based on imprinting the coherent properties of a light/optical source onto the matter to be controlled.[1,2] With the experimental realization of Bose–Einstein condensation,[3–6] a new source of coherent matter waves has become potentially available. The present paper explores the direct employment of a matter wave coherent source to achieve the goal of coherent control of a chemical reaction.

The utilization of a matter wave source depends on the experimental ability to direct and shape the matter waves from a Bose–Einstein condensation (BEC). The waves in a BEC trap constitute a single many-body matter wave function which is an analog of a photon field in an optical cavity. An output coupler termed *atom laser* transforms the condensate into a source of either pulsed or continuous coherent matter.[7–13] We propose to employ this matter wave for a surface mediated chemical reaction carried out by a two-pulse atomic coherent control (2PACC) spectroscopy. The present paper elaborates on previous preliminary studies (see Refs. 14, 15).

BEC has been accomplished for a growing list of atoms {^{133}**Cs** (Ref. 16), ^{87}**Rb** (Ref. 3), ^{85}**Rb** (Ref. 17), ^{23}**Na** (Ref. 4), ^{7}**Li** (Refs. 5, 6, 18), ^{6}**Li** (Ref. 18), **K** (Ref. 19), **H** (Ref. 20) and metastable **He** (Refs. 21, 22)}. All of the above condensates and additional systems to be prepared are candidates for a source for a coherently matter wave.

The principle of interfering optical waves in a molecular framework has neatly been demonstrated by Scherer *et al.*[23,24] Using a sequence of two optical pulses, population is transferred from the ground to the excited electronic state in the iodine molecule. The first pulse promotes a portion of the wave function to the excited state, which then evolves in time. The second pulse, which is phase locked relative to the first one, excites an additional wave packet to the excited state. The intramolecular superposition of the two wave packets is subject to quantum interferences, either constructive or destructive. This gives rise to larger or smaller population on the excited state for a given time delay between the pulses. The outcome is then controlled by the optical phase difference between the two pulses and the evolution of the initial wave packet.[23–26]

The objective of the study is to control a bimolecular surface reaction using a coherent source of matter waves shaped as two phase-locked pulses. The target substrate is a stationary atom adsorbed on a surface. The outcome of the reaction is a desorbed molecule in the gas phase composed from one atom from the matter wave pulse and one surface atom. The method is therefore termed two-pulse atomic coherent control (2PACC) spectroscopy. The yield of the reaction is controlled by the time delay between the two atomic pulses and the relative phase between them.

The majority of studies in coherent control has concentrated on unimolecular processes. An exception is the study by Abrashkevish *et al.*,[27] which theoretically considered a 3D-atom–diatom reactive scattering process. The 2PACC spectroscopy is aimed at the more difficult task of controlling a bimolecular reaction described by $A+B\rightarrow C$.

In contrast to a two-pulse photon field, the matter waves are dispersive. This means that the source of the matter waves, the BEC condensate, has to be positioned very close to the target surface. Such a device is realized in the so-called atom chips[28–31] or surface microtraps.[32,33] In the atom chips, for example, the BEC has been placed a few hundred

---

[a] Electronic mail: solvejg@fh.huji.ac.il
[b] Electronic mail: ronnie@fh.huji.ac.il

microns above a metal surface.[29,31] The additional step required to realize the current proposal is a two-pulsed output coupler directing a coherent pulse of atoms toward the surface.

A coherent optical spectroscopy employed in surface science is two-photo emission (2PPE), which has served as the inspiration for the present proposed 2PACC. In 2PPE, two photons from a laser are applied to a surface with or without adsorbates. In 2PPE, the first optical pulse excites a surface electron to an intermediate level of either an image potential state or an unoccupied molecular orbital of the adsorbate. The second photon exploits this excitation to create a measurable outcome. The method has been used to characterize the energetics and dynamics of electrons, atoms, and molecules on surfaces.[34–40] The application of two laser pulses allows for probing the nuclear dynamics of the electronic states which could not be studied if only one pulse was applied. Recently, Petek *et al.*[37] have demonstrated that applying a sequence of phase-locked optical pulses coherently controls the motion of an alkali atom on the metal surface and thereby the desorption process.

The bimolecular surface mediated reaction to be controlled by the 2PACC spectroscopy is the Eley–Rideal reaction. The atomic pulses consist of a coherent atomic source of hydrogen or alkali atoms which collide with a hydrogen atom chemisorbed on a **Cu**(111) surface. The outcome is an ejected molecule in the gas phase of either $\mathbf{H}_2$ or an alkali hydride. It will be shown that the application of a second atomic pulse induces the matter wave interferences that enable enhancement or suppression of the desorbing flux of molecules relative to a single atomic beam experiment. The quantum interferences are controlled by the time delay and the relative phase between the two atomic pulses.

Theoretical studies of Eley–Rideal reactions have been performed by Jackson *et al.*[41–44] for an incident hydrogen atom beam interacting with various coated surfaces. They have observed that hot atom processes, where the impinging atom becomes trapped onto the surface, play an important role. The trapped atoms can react with the adsorbate or they can eventually dissipate enough energy through collisions with the adsorbates to become immobile. These dissipative forces cause decoherence and therefore will suppress the 2PACC control. In this paper the energy and charge transfer between the surface and the adsorbates are not included.

The dynamics of the 2PACC spectroscopy model is explored by solving the time-dependent Schrödinger equation by a Newtonian propagation method.[45] The matter wave pulses are presented by two phase related Gaussian-type wave packets. The atomic and molecular as well as their interactions with the surface are described in a diabatic framework.

The methodology of the 2PACC spectroscopy is presented in Sec. II. In Sec. III the dynamics of 2PACC is presented. In Sec. IV two simulations of 2PACC spectroscopy are studied, one with a hydrogen source and another with a lithium atom laser, both impinging on a **Cu** surface with chemisorbed hydrogen atoms. Conclusions and a general outlook are presented in Sec. V.

II. THE MODEL

The target of control is the Eley–Rideal reaction described by

$$\mathbf{Y}+\mathbf{H}/\mathbf{Cu}(111)\rightarrow\mathbf{YH}+\mathbf{Cu}(111). \tag{1}$$

The atom **Y** is from the atom laser source, which in the present model consists of either hydrogen or alkali atoms. The matter wave of **Y** is directed to a **Cu**(111) surface with low coverage chemisorbed hydrogen atoms. When the wave function of **Y** overlaps with that of the adsorbed atom, interaction is expected, leading to a recombination that forms the **YH** molecule. If the newly formed molecule has sufficient energy it will eventually desorb from the surface to the gas phase. By shaping the wave function of **Y**, the yield of the desorbing molecules becomes controlled by constructive or destructive interference. The simplest controlled wave function is obtained by a sequence of two pulses where the time delay and relative phase are the control variables. It is anticipated that atom lasers will be able to produce such coherent matter wave pulses by an output coupler of a coherent source—the Bose–Einstein condensate (BEC). For example, a coherent atomic pulse can be realized by using an optical laser source to transfer the atom from a trapped (BEC) to an untrapped state (the atom laser). The relative phase between the two optical pulses can be utilized to phase lock the two pulses of the atom matter wave. A time delay between the two optical laser determines also the time delay between the two pulsed atomic laser. The coherent properties of interest are projected onto this wave function. In this study the wave function of an atom laser composed of a single atom is represented by two Gaussian wave functions with a well-defined time delay and phase. Other pulse shapes would lead to similar results provided that the time delay and relative phase between the two pulses are the same.

The binding energy for a hydrogen atom on a **Cu**(111) surface is roughly 2.4 eV. Since the bond energy of $\mathbf{H}_2$ is approximately twice this value, the reaction is very exothermic. For this reason the desorbing molecule is expected to be vibrationally hot due to the large exothermicity. As one proceeds through the list of atoms $(\mathbf{Y}=\{\mathbf{H},\mathbf{Li},\mathbf{Na},\mathbf{K},\mathbf{Rb},\mathbf{Cs}\})$ the reaction changes from exothermic to endothermic. If the **Cu**(111) surface is replaced with an **Al**(110) surface all the reactions again become exothermic since the binding energy of the hydrogen on this surface is only 1.8 eV.[46]

The dynamics of the Eley–Rideal reaction is a six-dimensional quantum-mechanical problem. We assume translational and rotational invariance relative to the surface, and the motion of the atoms has been restricted to a collinear configuration normal to the surface. The problem is reduced to a two-dimensional quantum-mechanical problem. We consider the reaction between an impinging atom of mass m_y located at z_y and a target atom of mass m_h located at z_h which is initially adsorbed on a flat static surface. The coordinate set (z_h,z_y) is transformed to a new set of coordinates (r,Z), where $r=z_y-z_h$ is the intramolecular distance and $Z=(m_hz_h+m_yz_y)/M$ is the center of mass coordinate. The total and reduced mass of the system are denoted by M and μ, respectively. Considering other surface degrees of freedom, such as phonons and electron/hole pairs, they also can influence the outcome of Eley–Rideal reactions. But, in the present 2PACC context only coherent contributions are important; therefore, these incoherent surface degrees of freedom can be ignored. The signal as in 2PPE spectroscopy is the difference between the single- and two-pulse experiment; therefore, it excludes the incoherent processes.

A. Two-dimensional potential energy surfaces

To understand the dynamics of either a dissociation reaction of a diatomic or a recombination reaction of two atomic species on a surface, potential energy surfaces (PES) representing the physics of breaking and forming a chemical bond is required. A comprehensive overview of the historical development of potential energy surfaces is given in Ref. 47.

An electronic structure model for the dissociation/recombination of the H_2/Cu system has been suggested by Holloway and co-workers.[48,49] Their model is based on a small complex of the form $\mathbf{Cu_2H_2}$ in a planar C_{2v} geometry. The intramolecular coordinates are r, which is the distance between the two hydrogen atoms, and Z, the distance between the midpoint of **H–H** and **Cu–Cu**. For large value of Z there is no interaction between the two units, **H–H** and **Cu–Cu**, meaning that each unit has a separate set of fully occupied molecular orbitals. As Z decreases the two units approach each other, the orbitals with similar symmetry with respect to the bond center mix, e.g., the parallel-bonding orbital of **H–H** and **Cu–Cu** interfere with the parallel antibonding of **Cu–H**. Due to these interactions the orbital energies shift. This causes a crossing between the ''parallel'' and ''perpendicular'' orbitals, with the result that the **H–Cu** bonding becomes energetically favorable.

The PES of the reactant surface has been constructed from a Morse potential describing the hydrogen–hydrogen bond and a repulsive potential as the hydrogen molecule approaches the surface. In the product channel the two separated hydrogen atoms are chemisorbed on the surface; this bond is described by a Morse potential. The hydrogen–hydrogen repulsion on the surface is represented by an exponential repulsive potential.

In the diabatic representation, the potential is represented by a 2×2 $\boldsymbol{V}$ matrix

$$\boldsymbol{V}(r,Z)=\begin{bmatrix}\boldsymbol{V}_{RR}(r,Z) & \boldsymbol{V}_{RP}(r,Z)\\ \boldsymbol{V}_{PR}(r,Z) & \boldsymbol{V}_{PP}(r,Z)\end{bmatrix}. \tag{2}$$

The diagonal elements are the potential energy surfaces of the reactant and the product states and the off-diagonal elements is the nonadiabatic couplings between them. Upon diagonalization of the 2×2 $\boldsymbol{V}$ matrix two new adiabatic PES are obtained. In the previous studies of Eley–Rideal reactions the adiabatic PES has been used. We will briefly discuss the idea behind them.

Jackson *et al.*[41,43,50] used the London–Eyring–Polanyi–Sato (LEPS) potential energy surface for modeling the Eley–Rideal reactions. The LEPS potential is given by

$$V=U_m+U_a+U_b\pm\sqrt{A_m^2+[A_a+A_b]^2-A_m[A_a-A_b]}, \tag{3}$$

where U and A are the Coulomb and exchange contributions, respectively. The intramolecular contributions are denoted U_m and A_m, whereas the other terms describe the atomic interactions with the surface. Here, only the lowest adiabatic PES are considered. The PES of the molecule as well as the interactions between the surface and a single atom have been calculated by density functional theory (DFT). They have been fitted to the functional forms, U and A, which are based on Morse-type attractive and repulsive terms which decay exponentially with increasing distances. Surface effects have been introduced through expanding the Morse parameters representing the surface in a Fourier series of the reciprocal lattice vectors.

The LEPS potential is a member of a class of diatomic in molecules (DIM) potential forms. For surface reactions, an extension called embedded diatomic in molecules (EDIM) has been developed. The model was originally developed by Truong *et al.*[51] and recently used for the description of the motion of N_2 on a ruthenium surface.[52] In the EDIM the intramolecular interactions are modeled by Morse and anti-Morse potentials which represent the singlet and triplet electronic state of the diatomic molecule in the gas phase. The interaction between the atoms in the gas phase and the surface is modeled by an embedded atom model (EAM), in which the atom experiences an average charge density from the surface.

In the 2PACC spectroscopy the coherent properties of the encounter is intricate; therefore, the Born–Oppenheimer approximation in which the reaction takes place on a single potential energy surface has to be replaced with a nonadiabatic framework. In the 2PACC dynamics a diabatic frame is chosen consisting of two potential energy surfaces. Specifically, for the Eley–Rideal reaction the diabatic PES are constructed from two atomic or one molecular chemical species interacting with the surface. In the reactant channel the interaction between the stationary hydrogen atom and the surface is strong due to a chemical bond. We are using a semiempirical functional form for the PES. The impinging atom experiences a repulsive force from the adsorbed atom as well as a long-range attraction from the surface due to polarization forces. In the product channel the newly formed molecule is attached to the surface by a weak bond induced by the polarization forces between the surface and the molecule. The PES for the reactant and product channels have the following functional forms:

$$\boldsymbol{V}_{RR}(r,Z)=V_{HM}^R+V_{YM}^R+V_{YH}^R, \tag{4}$$

$$\boldsymbol{V}_{PP}(r,Z)=V_{YH-M}^P+V_{YH}^P, \tag{5}$$

where the index **M** represents the interactions with the surface. The last terms of Eqs. (4)–(5) represent the intramolecular interaction between the two gas-phase atoms, **H** and **Y**. The other terms represent the interaction between an atom or a molecule with the surface. In the following section we will discuss each of the individual terms in the reactant and product PES.

1. Intramolecular interactions

Asymptotically, the intramolecular interaction potentials, V_{YH}^R and V_{YH}^P, in the reactant and product channels become the triplet and singlet electronic states of the molecule, **YH**, when both atoms are far from the metal surface. The PES of the alkali hydride molecule was based on the intramolecular gas-phase singlet and triplet electronic states which have been evaluated by a multiconfiguration self-consistent field calculation by Geum *et al.*[53] These potentials have been fitted to a cubic spline interpolation function.

For the hydrogen molecule the singlet and triplet PES are given by a Morse and an anti-Morse potential

$$V^P_{HH}(r,Z)=D_{HH}([1-e^{\{-\alpha_{HH}(Z)(r-r^e_{HH}(Z))\}}]^2-1),$$

$$V^R_{HH}(r,Z)=\frac{1}{2}\frac{1-\Delta}{1+\Delta}D_{HH}([1+e^{\{-\alpha_{HH}(Z)(r-r^e_{HH}(Z))\}}]^2-1).$$

The dissociation energy of the hydrogen molecule is denoted D_{HH} and $(1-\Delta)(1+\Delta)$ is the Sato factor. The equilibrium distance between the two hydrogen atoms, r^e_{HH}, and the coupling strength, α_{HH}, have been obtained as a function of Z by an interpolation between values for the gas phase to ones for the adsorbate

$$\begin{aligned}&\alpha_{HH}(Z)=\alpha^{ad}_{HH}\quad \text{for}\quad Z\leqslant Z_e\\&\alpha_{HH}(Z)=\alpha^{g}_{HH}-(\alpha^{g}_{HH}-\alpha^{ad}_{HH})\Gamma_4(Z,Z_e,2b_{HM})\\&\qquad\qquad \text{for}\ \ Z>Z_e,\end{aligned}\tag{6}$$

and

$$r^e_{HH}(Z)=r^g_e-(r^g_e-r^{ad}_e)\Gamma_4(Z,Z_e,2b_{HM}).\tag{7}$$

The superscripts g and ad indicate the gas phase and the adsorbed state. Table I gives the parameters used for the PES for a **Cu**(111) surface covered by a hydrogen atom adsorbed on the hollow site.

2. Surface interactions

In the product channel a molecule (**YH**) is formed and eventually transferred to the gas phase. The molecule is coupled to the surface by a weak bond induced by the polarization forces. The interaction potential, V^P_{YH-M}, is represented as a sum of two terms—a short-range repulsive term and a weak long-range attraction between the molecule and the surface

$$V^P_{YH-M}=A_Me^{(-b_MZ)}-\frac{C_M}{Z^3}(1-\Gamma_4(Z,0,2b_M)).\tag{8}$$

The incomplete gamma function which turns off the attraction as the **Y** atom approaches the surface is given by

$$\Gamma_m(x,x_0,a)=\sum_{k=0}^{k=m}\frac{a(x-x_0)^k}{k!}e^{(-a(x-x_0))}.\tag{9}$$

The parametrization of the physisorption of the molecular interaction with the surface has been chosen such that the minimum energy, e.g., the physisorption energy, is observed at $Z_e=(r^e_{HM}+m_yr^e_{YH})/M$. The location of the minimum energy is moved further away from the surface as the mass of the impinging atom increases. As **Y** becomes heavier, the polarization force between the surface and the alkali atom increases; thereby, the binding energy of the physisorption bond becomes stronger. The amplitudes of the repulsion, A_M and attraction, C_M increase as one proceeds down the list of atoms, {**H**,**Li**,**Na**,**K**,**Rb**,**Cs**}. The coupling strength, b_M, is inversely proportional to Z_e. The parameters are constructed so that the physisorption energy of **YH** increases slightly as one proceeds down the list of atoms {**H**,**Li**,**Na**,**K**,**Rb**,**Cs**}. The physisorption potentials are shown in Fig. 1 and the parameters are given in Table I.

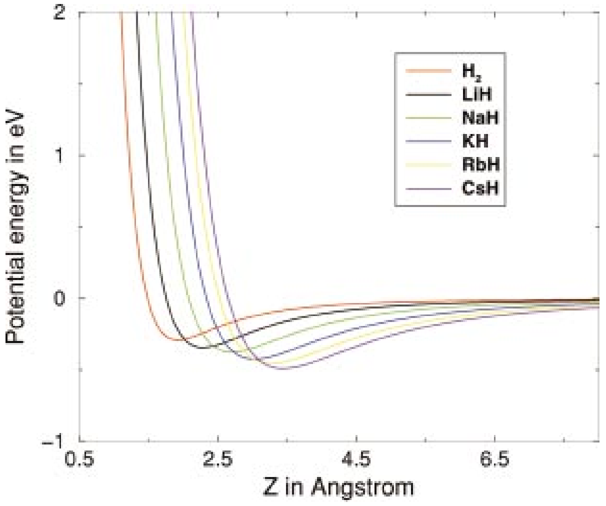

FIG. 1. (Color) The potential energy surface representing the physisorption of a hydrogen or an alkali hydride molecule on a **Cu**(111) surface is shown as a function of the distance between the surface and the mass center of the diatomic.

To model the interaction between the impinging atom in the reactant channel, a physisorption potential has been used. The same set of parameters for the atomic interaction as for the molecular physisorption interactions has been chosen but the coordinate, Z, in Eq. (8) is replaced by the location of the impinging atom, z_y.

In the reactant channel the interaction between the chemisorbed atom and the surface is described by a Morse potential

$$V^R_{HM}=D_{HM}([1-e^{(-\alpha_{HM}(z_h-z^e_{HM}))}]^2-1),\tag{10}$$

where D_{HM} is the dissociation energy of the atom–metal bond and z^e_{HM} is the equilibrium bond length. The parameters are given in Table I for a hydrogen atom adsorbed at the hollow site of a **Cu**(111) surface.

B. Wave function of the atomic pulse

Initially, when the impinging atom is far away from the surface and the adsorbed atom, the wave function representing the outcome of the total system is written as a product of a wave function on each atom

$$\begin{aligned}&\Psi_{\text{atom}}(r,Z)=N\psi_h(z_h,z_y=z_s)\psi_y(z_y)e^{ik_yz_y};\\&\psi_y(z_y)=e^{-(z_y-z_s)^2/\sigma_y},\end{aligned}\tag{11}$$

where N is a normalization factor. The wave function of the adsorbed atom, ψ_h, was chosen as the lowest energy eigenstate of the PES of the reactant channel along the one-dimensional path with a fixed distance, z_s, between the approaching atom and the surface. Considering only the lowest

TABLE I. The parameters for PES for the Eley–Rideal reaction on a **Cu**(111) surface. The hydrogen atom is chemisorbed on a hollow site of the surface.

Hydrogen molecule	$D_{HH}=4.505$ eV[a]	$Z_e=2.0$ Å	$\Delta=0.2$
	$r_e^{ad}=0.741$ Å[a]	$r_e^g=0.754$ Å[b]	
	$\alpha_{HH}^g=2.2$ Å^{-1}	$\alpha_{HH}^{ad}=2.11$ Å^{-1}	
Chemisorption	$D_{HM}=2.334$ eV[a]	$z_{HM}^e=0.916$ Å[a]	$\alpha_{HM}=1.75$ Å^{-1}[a]
Physisorption	A_M/eV	b_M/Å^{-1}	C_M/eV Å^{-3}
H_2 or **H**	600	3.8	3.5
LiH or **Li**	650	3.15	7.0
NaH or **Na**	760	2.7	12.5
KH or **K**	850	2.4	20.0
RbH or **Rb**	930	2.23	27.0
CsH or **Cs**	950	2.1	34.0

[a] Reference 50.
[b] Reference 54.

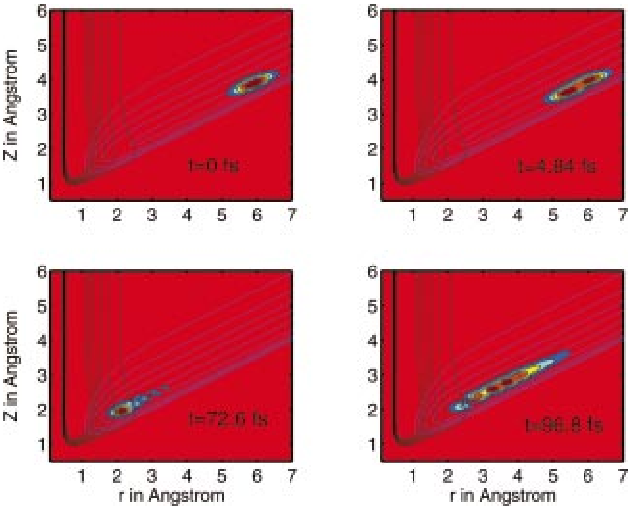

FIG. 2. (Color) The evolution of the wave packet ($|\boldsymbol{\Psi}_R|^2$) from an atom laser source applied to a **Cu**(111) surface coated with hydrogen atoms superimposed on the reactant potential energy surface. Snapshots are shown for a time delay of $\Delta t=4.84$ fs and the phase, $\theta=-\frac{1}{2}\pi$. The contour values of potential energy surfaces are -3, -2.5, -2, -1.5, -1, and -0.5 eV. The PES of the reactant and the product channels are shown with blue and black lines, respectively.

vibrational states would be sufficient since, in a given experimental situation, one would expect that the temperature of the surface is ultracold. The wave function of the approaching atom, ψ_y, is represented by a Gaussian wave function centered at $z_y=z_s$ and with a variance, σ_y. The momentum of the approaching atom is denoted by $k_y=\pm\sqrt{2m_yE/\hbar^2}$, which is related to the energy E of the propagating atom laser. The sign of the momentum operator determines the orientation of the atom laser: For negative momentum, the atom moves toward the surface. The variance is related to the dispersion of the atom laser.

III. 2PACC DYNAMICS

The 2PACC spectroscopy of an Eley–Rideal reaction consists of the dynamics on the coupled reactant and product potential energy surfaces. The wave function of the system is described by the vector

$$\boldsymbol{\Psi}(r,Z,t)=\begin{pmatrix}\boldsymbol{\Psi}_R(r,Z,t)\\ \boldsymbol{\Psi}_P(r,Z,t)\end{pmatrix}, \tag{12}$$

where the wave functions in the reactant and product channels are denoted by the index $\{R,P\}$. The Hamiltonian of the system is represented by

$$\begin{aligned}\boldsymbol{H}(r,Z)&=\boldsymbol{T}(r,Z)+\boldsymbol{V}(r,Z)\\ &=\begin{bmatrix}\boldsymbol{T}_{RR}(r,Z) & \mathbf{0}\\ \mathbf{0} & \boldsymbol{T}_{PP}(r,Z)\end{bmatrix}\\ &\quad+\begin{bmatrix}\boldsymbol{V}_{RR}(r,Z) & \boldsymbol{V}_{RP}(r,Z)\\ \boldsymbol{V}_{PR}(r,Z) & \boldsymbol{V}_{PP}(r,Z)\end{bmatrix}.\end{aligned} \tag{13}$$

The diagonal elements of the Hamiltonian have the following form:

$$\begin{aligned}\boldsymbol{H}_{ii}(r,Z)&=\boldsymbol{T}_{ii}(r,Z)+\boldsymbol{V}_{ii}(r,Z)\\ &=-\frac{\hbar^2}{2M}\frac{\partial^2}{\partial Z^2}-\frac{\hbar^2}{2\mu}\frac{\partial^2}{\partial r^2}+\boldsymbol{V}_{ii}(r,Z),\\ &\quad i=\{R,P\},\end{aligned} \tag{14}$$

where the first two terms are the kinetic energy operator for the two degrees of freedoms (r and Z) and the last term is the potential energy function which was described in Sec. II A. The off-diagonal elements of the Hamiltonian represent the nonadiabatic coupling between the two channels, which are described by

$$\boldsymbol{V}_{RP}(r,Z)=\boldsymbol{V}_{PR}(r,Z)=\beta e^{-(r-r_{YH}^e)^2}e^{-Z}, \tag{15}$$

where β is the nonadiabatic coupling strength and r_{YH}^e is the equilibrium distance between the two atoms in the singlet molecular PES. This representation ensures that the electron density of the metal decays exponentially outside the surface into the vacuum. The nonadiabatic coupling strength, β, was assigned the value 0.027 eV in all calculations. Changing β will only scale the total reaction yield. It is important to note that the adiabatic PES of the Eley–Rideal reaction which have been used by Jackson *et al.*[41–44] can be obtained by diagonalization of this 2×2 $\boldsymbol{V}$ matrix.

The dynamics of the 2PACC was followed by solving the time-dependent two-channel Schrödinger equation, which is given by

$$i\hbar\frac{\partial\boldsymbol{\Psi}}{\partial t}=\boldsymbol{H}\boldsymbol{\Psi}. \tag{16}$$

In the two-pulse atomic coherent control (2PACC) spectroscopy the first atom laser represented by the wave packet [Eq. (11)] is initialized at the reactant PES at a time $t=0$, e.g.,

$$\boldsymbol{\Psi}(r,Z,0)=\begin{pmatrix}\Psi_{\text{atom}}(r,Z)\\ 0\end{pmatrix}. \tag{17}$$

This initial wave packet evolves in time and after a time delay, Δt, the second atom pulse is introduced given by

$$\Psi_{\text{atom},2}(r,Z)=\Psi_{\text{atom}}(r,Z)\exp(-i\theta), \tag{18}$$

where $\theta\in[-\pi;\pi]$ is the relative phase between the two atomic pulses that describes the coherence between them. As

TABLE II. Computational parameters for the wave packet propagation of the 2PACC dynamics.

Time step	$\delta t=0.097$ fs
Propagation time	$t_{\max}=484$ fs
Time steps	$N_t=5000$
Grid points along r	$N_r=256$
Grid spacing along r	$\Delta r=0.0529$ Å
Grid starts at	$r_{\min}=0.0529$ Å
Grid points along Z	$N_Z=256$
Grid spacing along Z	$\Delta Z=0.0529$ Å
Grid starts at	$Z_{\min}=0.0529$ Å
Variance	$\sigma_y=0.280$ Å^2
Initial position	$z_s=6.82$ Å
Momentum	$k=9.45$ Å^{-1}
Absorbing potential	$\Delta_r=\Delta_Z=1.32$ Å $V_0=0.000\,27$ eV
Nonadiabatic coupling	$\beta=0.027$ eV
Dividing flux line	$Z_{\text{flux}}=5.24$ Å

the wave packet propagates, population is transferred from the reactant to the product PES through the nonadiabatic coupling.

A. Computational method

The wave function is represented on a two-dimensional grid. First, the wave function of the chemisorbed hydrogen was calculated. Using an imaginary time propagation[55] the one-dimensional wave function of the hydrogen atom, ψ_H along the line with a fixed distance between the approaching atom and the surface, $z_y=6.8$ Å, has been relaxed to its vibrational ground state. Representing the wave function of the impinging atom as a Gaussian wave function, the total wave packet Eq. (11) is then initialized.

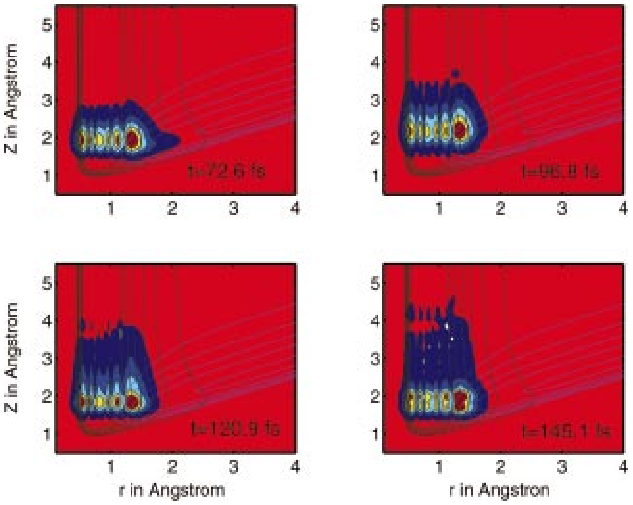

FIG. 3. (Color) The evolution of the wave packet on the product channel ($|\boldsymbol{\Psi}_P|^2$) are shown for time delay of $\Delta t=4.84$ fs and phase, $\theta=-\frac{1}{2}\pi$. Notice the exciting wave packet on the reactant channel at 145.1 fs. Parameters used for this calculation are given in Fig. 2.

The dynamics of the 2PACC is obtained by propagating the initial wave function by $\exp(-i\boldsymbol{H}t)\psi(0)$, in which the time-evolution operator $\exp(-i\boldsymbol{H}t)$ is expanded by Newtonian interpolation polynomials with Chebychev sampling points.[56] The kinetic energy operator has been evaluated using the fast Fourier transformation technique.[56,57] The parameters used in the wave packet propagation are displayed in Table II.

The scattered wave function is removed at large values of r and Z by complex absorbing potentials[58] which prevent reflection and transmission at the end of the grid. The overall potential can be written as

$$\begin{aligned} V(r,Z) &= V(r,Z)+V_{\text{abs}}(r)+V_{\text{abs}}(Z) \ \text{ if } \ r-\Delta_r\leqslant r\leqslant r_{\max} \ \text{ and } \ Z-\Delta_Z\leqslant Z\leqslant Z_{\max} \\ &= V(r,Z)+V_{\text{abs}}(r) \ \text{ if } \ r-\Delta_r\leqslant r\leqslant r_{\max} \ \text{ and } \ Z\leqslant Z-\Delta_Z = V(r,Z)+V_{\text{abs}}(Z) \ \text{ if } \ r\leqslant r-\Delta_r \ \text{ and } \ Z-\Delta_Z\leqslant Z\leqslant Z_{\max} \\ &= V(r,Z) \ \text{ if } \ r\leqslant r-\Delta_r \ \text{ and } \ Z\leqslant Z-\Delta_Z, \end{aligned} \tag{19}$$

where the complex potential is given by $V_{\text{abs}}(r)=iv_0(r-(r_{\max}-\Delta_r))^2$. The same functional form is used for Z. $r_{\max}$ is the last grid point and Δ_r is the interval where the complex potential is applied.

As the wave function is evolving from the entry/reactant channel, the nonadiabatic coupling term is responsible for transferring the amplitude between the two diabatic surfaces. Eventually the molecule desorbs from the metal surface. This leads to an outgoing flux in the exit/product channel. The probability of a **YH** molecule to escape from the metal surface is obtained via a flux-resolved analysis carried out at an asymptotic value of $Z=Z_{\text{flux}}=5.24$ Å. The total accumulated desorbing flux which is the predicted 2PACC signal is computed by

$$\begin{aligned} F &= \sum_i^{N_t} J(t_i)\,\delta t \\ &= \frac{\delta t}{M}\sum_i^{N_t} \ \text{Im}\left[\int dr\,\boldsymbol{\Psi}_P^*(r,Z_{\text{flux}},t_i)\frac{\partial\boldsymbol{\Psi}_P(r,Z,t_i)}{\partial Z}\bigg|_{Z=Z_{\text{flux}}}\right], \end{aligned} \tag{20}$$

where the derivative is evaluated with a Fourier transform. The integrated flux has been determined as a function of the time delay, Δt, and the phase relation, θ, between the two atom laser pulses.

Furthermore, the accumulated flux current can be evaluated for each of the vibrational states along the dividing line

$$
\begin{aligned}
P_n &= \sum_i^{N_t} j_n(t_i)\,\delta t \\
&= \frac{\delta t}{M} \sum_i^{N_t} \operatorname{Im}\left[\Psi_n^*(Z_{\text{flux}},t)\, \frac{\partial \Psi_n(Z,t)}{\partial Z} \bigg|_{Z=Z_{\text{flux}}} \right], \qquad (21)
\end{aligned}
$$

where j_n is the probability current for the wave packet to go into the nth vibrational state. Here, $\Psi_n(Z,t)$ is the projection of the wave function onto the vibrational eigenstates, χ_n, along the dividing line

$$\Psi_n(Z,t) = \int dr\, \chi_n^*(r) \Psi_P(r,Z,t). \qquad (22)$$

The vibrational eigenstatates have been calculated by imaginary time propagation. (See the Appendix for further details.)

IV. RESULTS AND DISCUSSION

The 2PACC of a hydrogen source is compared to that of a lithium atom laser source impinging on a surface with chemisorbed hydrogen atoms. The evolution of the wave packet on the reactant and the product channel is presented. The 2PACC signal and the vibrational analysis of the desorbing molecule are displayed. The control parameters are the time delay and relative phase between the two atom laser pulses.

A. H+H/Cu(111)

The dynamics of the 2PACC spectroscopy is demonstrated for a hydrogen atom laser source impinging on a **Cu**(111) surface coated with hydrogen atoms. Compared to earlier calculations[14,15] the grid spacing in both degrees of freedom (r,Z) was reduced by a factor of 2. The initial starting position of the wave function was $z_s = 6.8$ Å compared to 13.6 Å in the earlier calculations. At the shorter distance the interactions between the impinging atom and the adsorbate and the surface is still negligible.

In Figs. 2 and 3 snapshots of the evolution of the wave packet on the reactant and the product surfaces are shown for $\theta = -\frac{1}{2}\pi$ and $\Delta t = 4.84$ fs. First, the initial wave packet [Eq. (11)] is generated and this atom laser pulse evolves in time. The energy of the initial wave packet is -2.3 eV and the impinging atom has a kinetic energy of 0.2 eV. After the specified time delay a wave packet—the second atom laser pulse—is placed in the original position of the first wave packet (see the second snapshot of Fig. 2). The relative phase between the two wave packets at the initial position may be different, e.g., $\theta \neq 0$. The wave function which resembles the two atom laser pulses propagates toward the nonadiabatic region where the reactant and the product surfaces intersect. As the wave packet enters the nonadiabatic region a part of the wave function is transferred to the molecular state where it can exit. This means that the approaching hydrogen atom has reacted with the adsorbed hydrogen and a H_2 molecule is formed. The nonreactive part of the wave function collides with the adsorbed hydrogen atoms. Either it scatters back to the gas phase or it gets trapped on the surface due to the weak polarization forces between the impinging atom and the surface (physisorption).

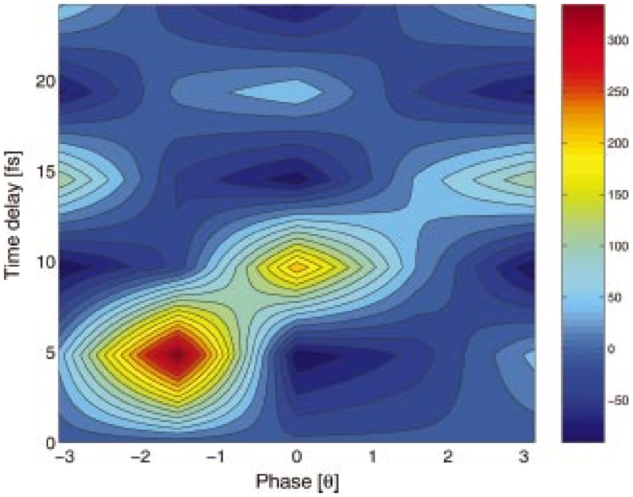

FIG. 4. (Color) The 2PACC signal of a hydrogen atom laser impinging on a surface with chemisorbed hydrogen atoms relative to the outcome for one pulse (in %). The signal is shown as a function of the time delay (in fs) and relative phase (θ) between the two atomic pulses for an initial wave packet with energy -2.3 eV. The predicted 2PACC signal is calculated from the integrated flux along a dividing line on the product channel at $t = 484$ fs. Areas of enhancement are in red and those of depletion in blue.

The population which is transferred through the nonadiabatic coupling to the product channel builds up slowly as a function of time. In the beginning the newly formed hydrogen molecule is physisorbed on the surface. That is, it is trapped in the potential well. Later a fraction of the wave function exits the channel and the hydrogen molecule desorbs from the surface to be detected in the gas phase. The desorbing molecule is vibrationally excited. The node structure of the exiting wave function shows that the hydrogen molecule desorbs in the fifth vibrational state $(\nu = 4)$. This observation will be verified by a vibrational analysis.

The 2PACC signal, which is the difference between a one-pulse and a two-pulse desorbed molecular outcome, is calculated from the total integrated flux at $t = 484$ fs. Figure 4 shows the 2PACC signal as a function of time delay and relative phase between the two pulses. The amount of control of the 2PACC signal demonstrated in this model is an enhancement of 350% for $\theta = -\frac{1}{2}\pi$ and $\Delta t = 4.84$ fs relative to one atomic pulse compared with a suppression of 95% at $\theta = \pi$ and $\Delta t = 9.7$ fs.

The 2PACC signal shows a variation with respect to both control parameters, meaning that the outcome of the Eley–Rideal reaction is coherently controlled by the time delay and the relative phase between the two atomic pulses. The application of the second pulse creates a quantum interference with the first pulse. Such interferences are either constructive or destructive, resulting in increasing or decreasing the flux of the desorbing molecules in the product channel. The effect of these interferences can be visualized by considering the wave function just after the second atom pulse has been applied. In Fig. 5 the total wave packet is shown for $t = \Delta t = 14.5$ fs for different relative phases between the two atom laser pulses. An elongated structure of the wave packet immediately after the second pulse gives rise to destructive interference and decrease of the desorption yield, whereas a

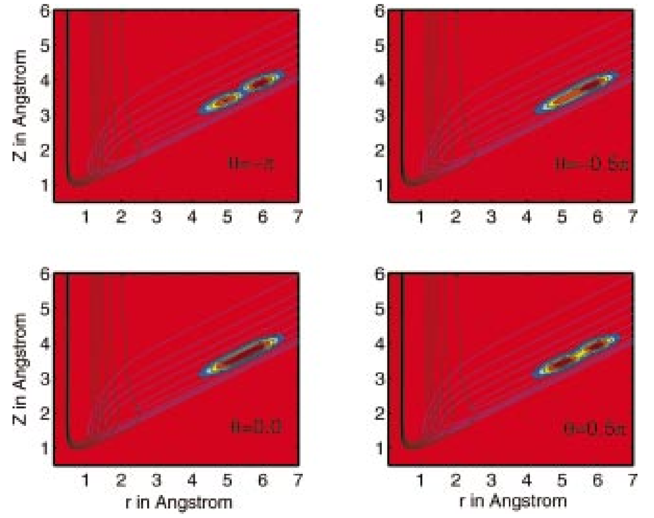

FIG. 5. (Color) The wave packet after the second atom laser pulse has been applied at $t=\Delta t=14.5$ fs for different relative phases between the two atomic pulses.

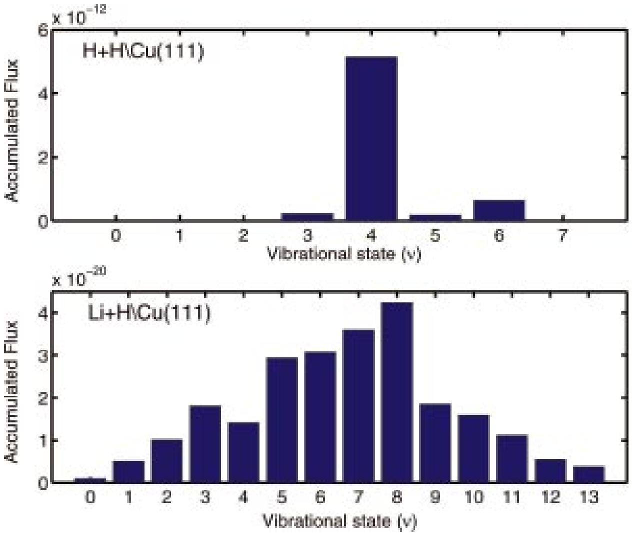

FIG. 6. (Color) The accumulated flux in each of the vibrational states for the one pulse experiment are shown for hydrogen (upper figure) and lithium (lower figure).

''node-like'' structure gives rise to constructive interference and an enhancement of the yield.

In Fig. 6 the accumulated flux in each vibrational state of desorbing hydrogen molecule is shown for a one-pulse experiment. The hydrogen molecule leaves the surface predominantly in the fifth lowest vibrational excited state ($\nu=4$). This observation agrees with the node structure of the leaving wave function on the product channel (see Fig. 3). Jackson *et al.*[44] also observed a vibrational distribution of desorbing hydrogen molecules centered around $\nu=4$ for an Eley–Rideal reaction of two hydrogen atoms on a Cu(111) surface in a collinear quantum-mechanical calculation.

The extent of control in the accumulated vibrational flux between the two- and one-pulse scenario is shown in Fig. 7. For all the calculations the vibrational distribution is centered around $\nu=4$. An enhancement of flux in the lowest vibrational states of the hydrogen molecule ($\nu\leqslant 3$) is correlated with an increases of the total 2PACC yield. On the other hand, an enhancement of the higher lying vibrational states ($\nu\geqslant 4$) is anticorrelated with the total 2PACC yield.

B. Li+H/Cu(111)

Next, the lithium with an adsorb hydrogen Eley–Rideal reaction on a **Cu**(111) surface is studied. A smaller probability of desorption for lithium hydride molecule is expected. This is due to the reduced energy difference between the product and the reactant and a stronger physisorption interaction between the surface and the lithium hydride. For a single matter wave pulse, the desorbing flux of lithium hydride is suppressed by 10^{-9} compared to desorption of hydrogen. The total energy of the initial wave packet is -2.4 eV, where the initial kinetic energy of the impinging atom is 0.027 eV.

The evolution of the wave packet on the reactant and the product PES is shown in Figs. 8 and 9. The dynamics of the 2PACC spectroscopy with a lithium atom laser is slower than the one for a hydrogen atom laser, since the mass of the impinging atom increases by almost a factor of 7. As the wave packet on the reactant channel approaches the metal surface, part of the population is transferred to the product channel. The magnitude of population transfer is much smaller for lithium than for hydrogen, as expected. The part of the wave packet on the reactant channel which does not react is primarily trapped on the surface due to polarization forces, and only a very small part of the wave function scatters back to the gas phase. The opposite was observed for the hydrogen case.

The predicted 2PACC signal is shown in Fig. 10 as a function of time delay and phase between the two pulses. For certain values of time delay and phase between the two pulses the second pulse induces large constructive interferences. These interferences enhance the probability of desorption for **LiH** by 2100% relative to a single-pulse experiment. The magnitude of coherent control of the formation of lithium hydride compared to recombination of two hydrogen molecule is mainly an energetic effect. The Eley–Rideal reaction with impinging lithium atoms is thermoneutral, whereas the recombination reaction with a hydrogen atom laser is highly exothermic. As a result, interference which is the source of control is enhanced.

The desorbing molecule, **LiH**, is vibrationally excited. This is because the bond length **LiH** is considerably longer than chemisorption bond between the hydrogen and the **Cu**(111) surface. Along the dividing line where the desorbing flux is collected, the 14 lowest vibrational eigenstates of the lithium hydride have been evaluated. For a single-pulse experiment (see Fig. 6) a broad distribution of the vibrational states with a maximum at $\nu=8$ is observed. In Fig. 11 the enhancement/suppression in the integrated vibrational flux relative to the single-pulse scenario is shown. The deviation in the integrated flux as a function of the phase reflects the 2PACC signal. If there is a large enhancement of the 2PACC signal, the accumulated flux in each vibrational state increases.

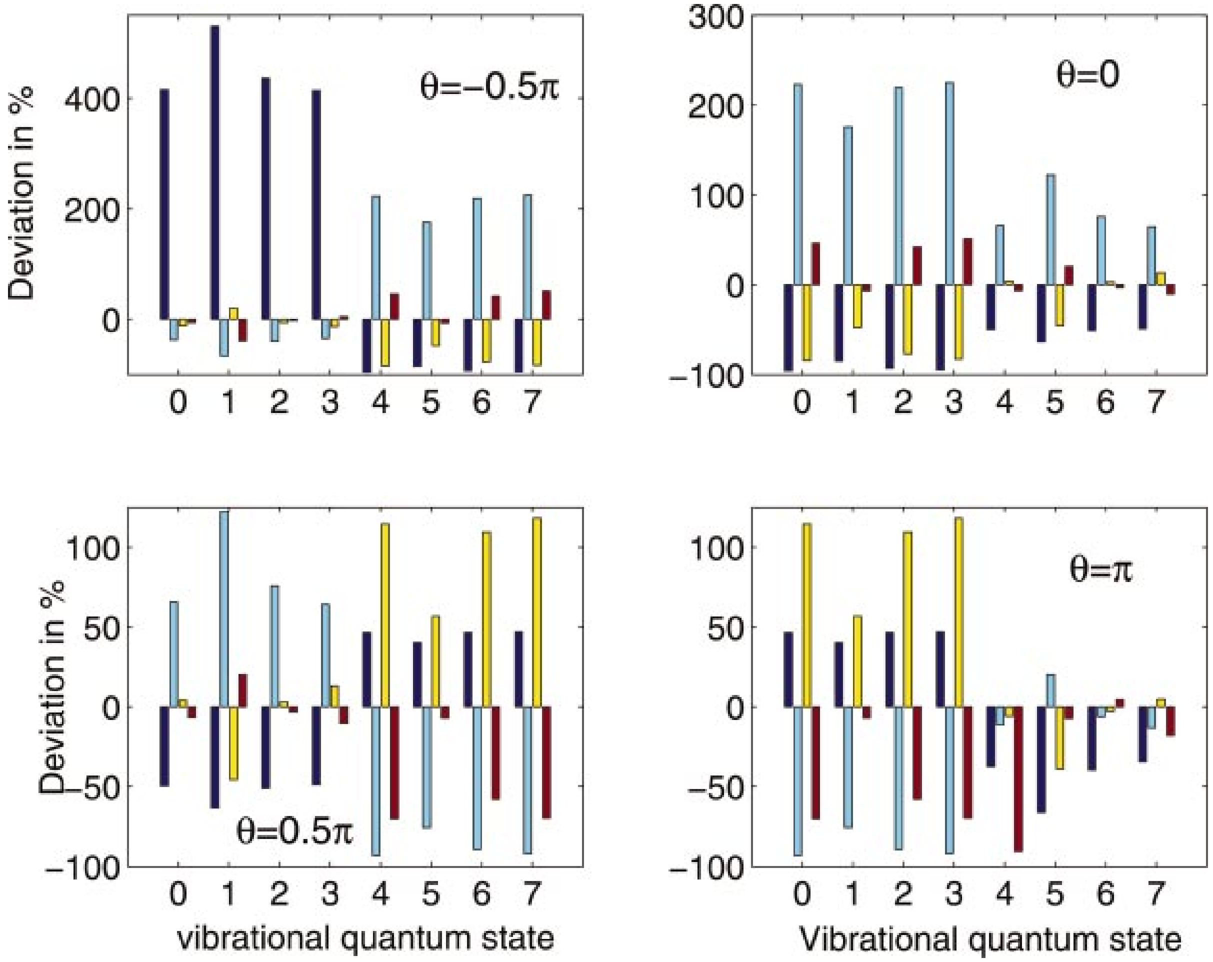

FIG. 7. (Color) The percentage deviation in the accumulated flux in the vibrational states from the one-pulse experiment are shown for four different relative phases (θ) between the two pulses. For each of the phases the accumulated fluxes are displayed for four time delays: (1) $\Delta t = 4.84$ fs (dark blue); (2) $\Delta t = 9.68$ fs (light blue); (3) $\Delta t = 14.52$ fs (yellow); and (4) $\Delta t = 19.35$ fs (red). The accumulated flux in each vibrational state for a one pulse experiment is shown in Fig. 6.

V. SUMMARY AND CONCLUSIONS

A two-pulse atomic coherent control (2PACC) spectroscopy has been presented in this study. The coherent properties of an atom laser have been used to control a surface mediated chemical reaction, $A+B\rightarrow C$, where the A wave function is generated from an atom laser and the target atom B is immobilized by the surface. Two atom laser pulses are applied creating an interference pattern with each other. These interferences are the essence of the coherent control of the chemical reaction. The two pulses are necessary since the initial relative phase between the atom A and atom B on the surface is arbitrary.[59,60] The two-pulse model is the simplest model for obtaining coherent control of the surface mediated reaction. The control knobs used were the time delay and a relative phase between two atom laser pulses. A significant enhancement of the 2PACC signal relative to single atom laser pulse was obtained.

The Eley–Rideal reaction forming $\mathbf{H}_2$ is highly exothermic, whereas the recombination reaction leading to **LiH** is almost thermoneutral. Using a coherent matter wave source enables us to coherently control the recombination reaction. The 2PACC spectroscopy opens up reaction channels which are almost closed to incoherent sources. The reaction yield by Eley–Rideal reaction of lithium atom laser with adsorbed hydrogen atom has been enhanced by more than 2100% compared to a one-pulse reference. Here, we manipulated the wave function of one atom transferred from a trapped state in the BEC to an untrapped and propagating state. The coherent properties of interest are projected onto this wave function. In this study, a double-Gaussian wave function was used where the source of coherent control is the time delay and relative phase between the two Gaussian wave functions. We could also have used a hyperbolic sine function for each pulse where we also can define a time delay and relative phase between the two pulses.

The 2PACC spectroscopy of an Eley–Rideal reaction could be realized by making an output coupler of the BEC in the atom chips[28–31] or surface microtraps.[32,33] Applying two phase-locked optical laser pulses to the BEC, a two-pulse matter wave is initialized. Schneider *et al.*[31] have designed their atom chip so that the BEC can be manipulated by coherent light. This design makes an output coupler for a BEC located close to a surface feasible. Proximity to the surface will also reduce the natural dispersion effect of the matter waves.

In analogy with the optical pulse shaper,[61,62] a more

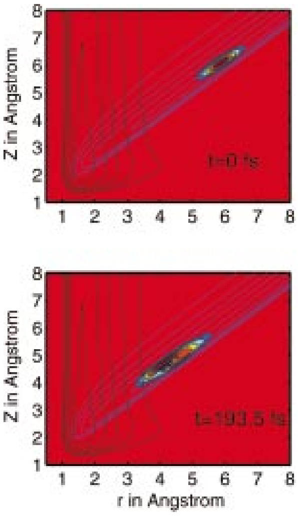

FIG. 8. (Color) Evolution of the wave packet on the reactant surface for the lithium atom laser impinging on a **H**/**Cu** surface. The time delay and the relative phase between the two atom laser pulses are $\Delta t = 9.7$ fs and $\theta = -\frac{1}{2}\pi$. The contours given for -3, -2.5, -2, -1.5, -1, and -0.5 eV for the potential energy surfaces of the product, and the reactant channels are shown with blue and black lines, respectively.

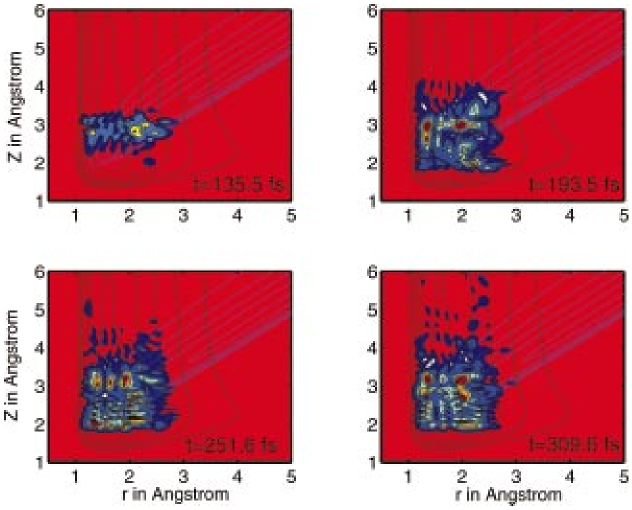

FIG. 9. (Color) Evolution of the wave packet on the product PES for lithium atom laser impinging on a **H**/**Cu** surface. The time delay and the relative phase between the two atom laser pulses are $\Delta t = 9.7$ fs and $\theta = -\frac{1}{2}\pi$.

elaborated matter wave pulse shaper would eventually lead to a reaction probability of one. Such a pulse shaper should have complete control of both amplitude and phase of the impinging wave packet. A more complex design of the wave function of the output coupler is under investigation. Shaping the incident wave function could further be used to direct the exiting molecule into a specific rovibrational state. The 2PACC spectroscopy could also be employed for endothermic reaction such as Eley–Rideal reaction between a adsorbed hydrogen atom and sodium (rubidium, cesium).

Additional coherent manipulations could be possible if the atomic matter wave pulse is replaced by a molecular pulse where the source is a molecular Bose–Einstein condensate. For a heterogeneous molecular matter wave the branching ratio between the two reaction channels could be controlled. From the perspective of coherent control methodology the current study demonstrates control of a recombination reaction. This is in contrast to optical coherent control, which has been almost exclusively limited to the control of unimolecular reactions such as photodissociation.

Control of a recombination reaction is another direction where both atoms come from the same BEC source. In this case their initial relative phase is well defined while the surface serves to break the symmetry. Since both sources are coherent the reaction product is also coherent. The ultimate goal is to design the wave functions of the atom lasers such that the reaction probability is unity for one specific rovibrational states of the product. This would lead to the formation of a stable molecular BEC. Control on these lines is under investigation.

ACKNOWLEDGMENTS

The authors would like to thank Christiane Koch for proofreading the manuscript. S.J. thanks Marie Curie Fellowship Organization. This work was supported by the Israel Science Foundation and the European Research and Training Network *Cold Molecules: Formation, Trapping and Dynamics*. The Fritz Haber Center is supported by the Minerva Gesellschaft für die Forschung, GmbH München, Germany.

APPENDIX: VIBRATIONAL EIGENSTATES

Vibrational eigenstates, χ_n, are solutions of the one-dimensional, one-channel, time-independent Schrödinger equation for a fixed distance, Z_{flux}, from the surface

$$\boldsymbol{H}_{PP}(r;Z_{\text{flux}})\chi_n(r;Z_{\text{flux}}) = E_n(Z_{\text{flux}})\chi_n(r;Z_{\text{flux}}). \tag{A1}$$

Asymptotically, when $Z_{\text{flux}} \to \infty$, the eigenstates represent the vibrational states of the diatomic molecule in the gas phase. The method for evaluating the eigenfunction is based on propagating a trial wave function according to the time-

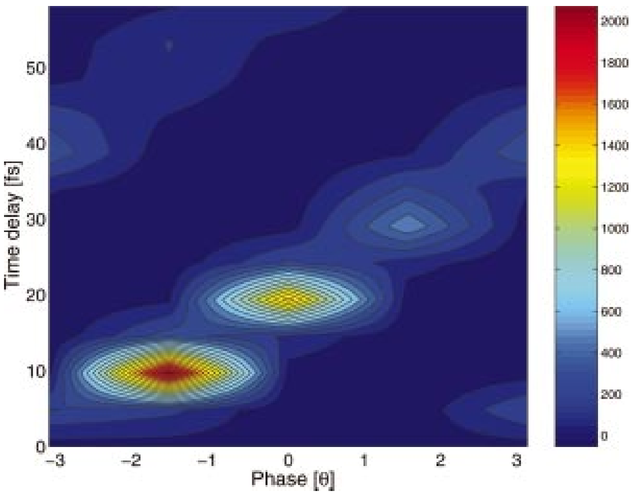

FIG. 10. (Color) The 2PACC signal. The enhancement relative to the output of a single pulse for lithium atom laser applied to a **H**/**Cu**(111) surface. The control parameters are the time delay and phase between the two pulse. The predicted 2PACC signal is calculated from the integrated flux along a divided line on the product channel at $t = 484$ fs. Areas of enhancement are in red and those of depletion are in blue.

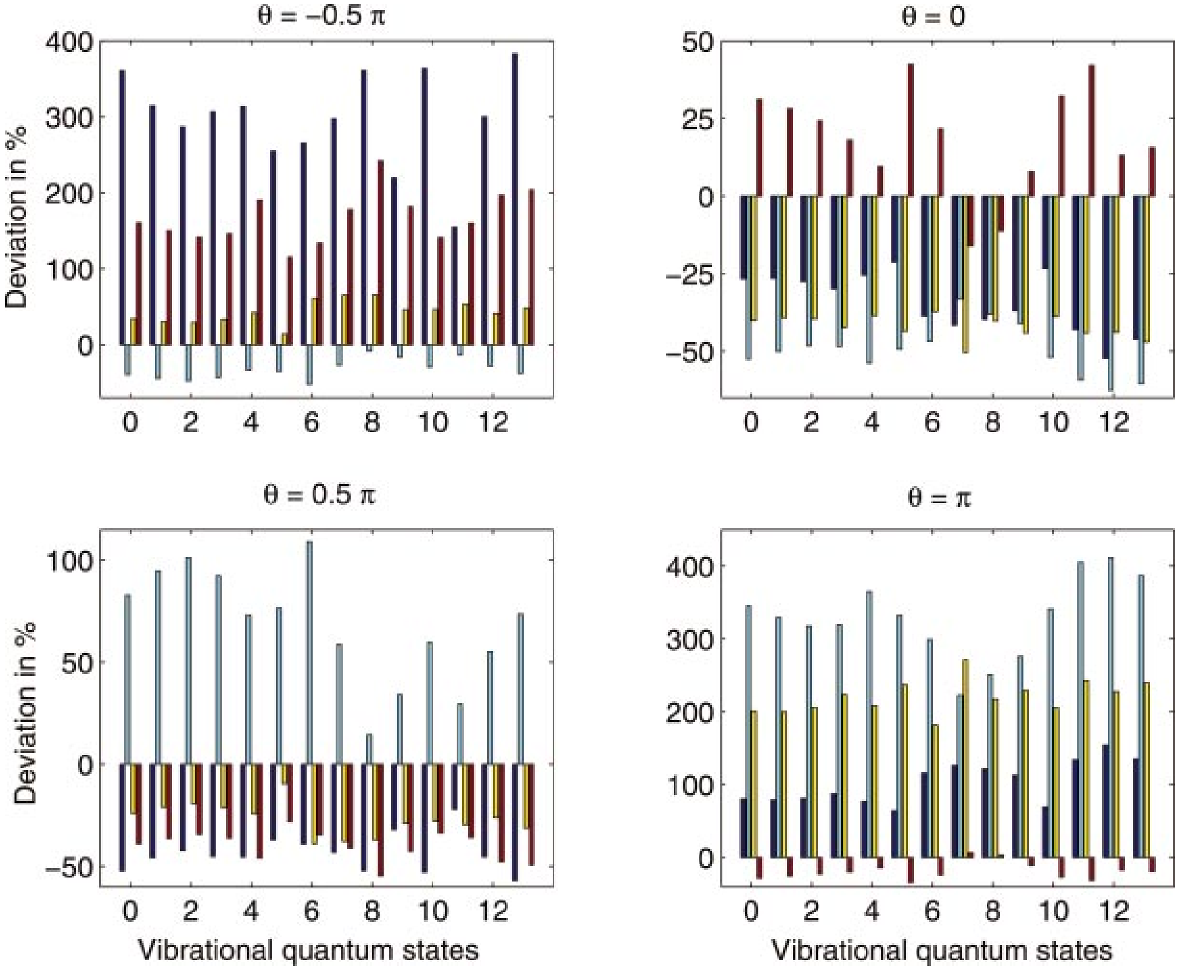

FIG. 11. (Color) The percentage deviation in the accumulated flux in the vibrational states relative to the single-pulse simulation. Four different relative phases (θ) between the two pulses are shown. For each of the phases the accumulated fluxes are displayed for four time delays: (1) $\Delta t = 38.7$ fs (dark blue); (2) $\Delta t = 43.5$ fs (light blue); (3) $\Delta t = 48.5$ fs (yellow); and (4) $\Delta t = 53.2$ fs (red). The accumulated flux in each vibrational state for the single pulse simulation is shown in Fig. 6.

dependent Schrödinger equation in imaginary time $\tau = it$. A Gaussian filter[63] has been used to project the eigenstates out in an energy region around an initial guess, ϵ

$$\chi_{\text{trial}}(r,\tau) = e^{-4(\boldsymbol{H}-\epsilon)^2\tau/\hbar\Delta E}\chi_{\text{trial}}(r,0). \tag{A2}$$

The parameter τ has the dimension of time, while ΔE is the energy range covered by the numerical procedure which appears as a scaling factor for the normalization of the Hamiltonian in the Newtonian time propagation. This procedure can be interpreted as a relaxation of the ground state of a modified Hamiltonian $\boldsymbol{H}^* = 4(\boldsymbol{H}-\epsilon)^2/\Delta E$. Convergence onto a specific target eigenstate can be estimated from the energy dispersion relation

$$D(\tau) = \sqrt{\langle\chi(\tau)|\boldsymbol{H}^2|\chi(\tau)\rangle - \langle\chi(\tau)|\boldsymbol{H}|\chi(\tau)\rangle^2}, \tag{A3}$$

which decreases uniformly by increasing the ‘‘purity’’ of an eigenfunction and vanishes in the limit of an exact eigenstate. If the energy dispersion, $D(\tau)$ is less than $1.0E$-6 the propagation is stopped and the wave function is a vibrational eigenstate of the diatomic molecule, χ_n, for a fixed distance to the surface.

[1] S. A. Rice, Nature (London) **409**, 422 (2001).
[2] R. J. Gordon and S. A. Rice, Annu. Rev. Phys. Chem. **48**, 601 (1997).
[3] M. H. Anderson, J. R. Matthews, C. E. Wieman, and E. A. Cornell, Science (Washington, DC, U.S.) **269**, 198 (1995).
[4] K. B. Davis, M.-O. Mewes, M. R. Andrews, N. J. van Druten, D. S. Durfee, D. M. Kurn, and W. Ketterle, Phys. Rev. Lett. **75**, 3969 (1995).
[5] C. C. Bradley, C. A. Sackett, J. J. Tollett, and R. G. Hulet, Phys. Rev. Lett. **75**, 1687 (1995).
[6] C. C. Bradley, C. A. Sackett, and R. G. Hulet, Phys. Rev. Lett. **78**, 985 (1997).
[7] M.-O. Mewes, M. R. Andrews, D. M. Kurn, D. S. Durfee, C. G. Townsend, and W. Ketterle, Phys. Rev. Lett. **78**, 582 (1997).
[8] B. P. Anderson and M. A. Kasevich, Science (Washington, DC, U.S.) **282**, 1686 (1998).
[9] E. W. Hagley, L. Deng, M. Kozuma, J. Wen, K. Helmerson, S. L. Rolston, and W. D. Phillips, Science (Washington, DC, U.S.) **283**, 1706 (1999).
[10] I. Bloch, T. W. Hänsch, and T. Esslinger, Phys. Rev. Lett. **82**, 3008 (1999).
[11] Y. L. Coq, J. H. Thywissen, S. A. Rangwala, F. Gerbier, S. Richard, G. Delannoy, P. Bouyer, and A. Aspect, Phys. Rev. Lett. **87**, 170403 (2001).
[12] M. Köhl, T. W. Hänsch, and T. Esslinger, Phys. Rev. A **65**, 021606 (2002).
[13] A. P. Chikkatur, Y. Shin, A. E. Leanhardt, D. Kielpinski, E. Tsikata, T. L. Gustavson, D. E. Pritchard, and W. Ketterle, Nature (London) **296**, 2193 (2002).
[14] S. Jørgensen and R. Kosloff, Surf. Sci. **528**, 156 (2003).
[15] S. Jørgensen and R. Kosloff, in *Interactions in Ultracold Gases: From Atoms to Molecules*, edited by M. Weidemüller and C. Zimmermann (Wiley, Berlin, 2003).

[16] T. Weber, J. Herbig, M. Mark, H.-C. Nägerl, and R. Grimm, Science (Washington, DC, U.S.) **299**, 232 (2003).
[17] S. L. Cornish, N. R. Claussen, J. L. Roberts, E. A. Cornell, and C. E. Wieman, Phys. Rev. Lett. **85**, 1795 (2000).
[18] F. Schreck, L. Khaykovich, K. L. Corwin, G. Ferrari, T. Bourdel, J. Cubizolles, and C. Salomon, Phys. Rev. Lett. **87**, 080403 (2001).
[19] G. Modugnu, G. Ferrari, G. Roati, R. J. Brecha, A. Simoni, and M. Inguscio, Science (Washington, DC, U.S.) **294**, 1320 (2001).
[20] D. G. Fried, T. C. Killian, L. Willmann, D. Landhuis, S. C. Moss, D. Kleppner, and T. J. Greytak, Phys. Rev. Lett. **81**, 3811 (1998).
[21] F. P. D. Santos, J. Léonard, J. Wang, C. J. Barrelet, F. Perales, E. Rasel, C. S. Unnikrishnan, M. Leduc, and C. Cohen-Tannoudji, Phys. Rev. Lett. **86**, 3459 (2001).
[22] A. Robert, O. Sirjean, A. Browaeys, J. Poupard, S. Nowak, D. Boiron, C. I. Westbrook, and A. Aspect, Science (Washington, DC, U.S.) **292**, 461 (2001).
[23] N. F. Scherer, A. J. Ruggiero, M. Du, and G. R. Fleming, J. Chem. Phys. **93**, 856 (1990).
[24] N. F. Scherer, R. J. Carlson, A. Matro, M. Du, A. J. Ruggiero, V. Romero-Rochin, J. A. Cina, and G. R. Fleming, J. Chem. Phys. **95**, 1487 (1991).
[25] R. Kosloff, A. D. Hammerich, and D. Tannor, Phys. Rev. Lett. **69**, 2172 (1992).
[26] A. Bartana, R. Kosloff, and D. Tannor, J. Chem. Phys. **99**, 196 (1993).
[27] A. Abrashkevich, M. Shapiro, and P. Brumer, Phys. Rev. Lett. **81**, 3789 (1998).
[28] M. P. A. Jones, C. J. Vale, D. Sahagun, B. V. Hall, and E. A. Hinds, quant-ph/0301018 2003.
[29] R. Folman, P. Krüger, C. Henkel, and J. Schmiedmayer, Adv. At., Mol., Opt. Phys. **48**, 263 (2002).
[30] W. Hänsel, P. Hommelhoff, T. W. Hänsch, and J. Reichel, Nature (London) **413**, 498 (2001).
[31] S. Schneider, A. Kasper, C. vom Hagen, M. Bartenstein, B. Engeser, T. Schumm, I. Bar-Joseph, R. Folman, L. Feenstra, and J. Schmiedmayer, Phys. Rev. A **67**, 023612 (2003).
[32] A. E. Leanhardt, A. P. Chikkatur, D. Kielpinski, Y. Shin, T. L. Gustavson, W. Ketterle, and D. E. Pritchard, Phys. Rev. Lett. **89**, 040401 (2002).
[33] H. Ott, J. Fortágh, G. Schlotterbeck, A. Grossmann, and C. Zimmerman, Phys. Rev. Lett. **87**, 230401 (2001).
[34] K. Geisen, F. Hage, F. J. Himpsel, H. J. Reiss, and W. Steinmann, Phys. Rev. Lett. **55**, 300 (1985).
[35] T. Fauster and W. Steinmann, in *Photonic Probes of Surfaces*, edited by P. Halevi (North-Holland, Amsterdam, 1995), Vol. 2, p. 347.
[36] C. B. Harris, N.-H. Ge, R. L. Lingle, J. D. McNeill, and C. M. Wong, Annu. Rev. Phys. Chem. **48**, 711 (1997).
[37] H. Petek and S. Ogawa, Annu. Rev. Phys. Chem. **53**, 507 (2002).
[38] I. L. Shumay, U. Höfer, C. Reuss, U. Thomann, W. Wallauer, and T. Fauster, Phys. Rev. B **58**, 13974 (1998).
[39] T. Vondrak, H. Wang, P. Winget, C. J. Cramer, and X.-Y. Zhu, J. Am. Chem. Soc. **122**, 4700 (2000).
[40] C. Gahl, K. Ishioka, Q. Zhong, A. Hotzel, and M. Wolf, Faraday Discuss. **117**, 191 (2000).
[41] X. Sha, B. Jackson, and D. Lemoine, J. Chem. Phys. **116**, 7158 (2002).
[42] B. Jackson and D. Lemoine, J. Chem. Phys. **114**, 474 (2001).
[43] D. V. Shalashilin, B. Jackson, and M. Persson, J. Chem. Phys. **110**, 11038 (1999).
[44] B. Jackson and M. Persson, J. Chem. Phys. **96**, 2378 (1992).
[45] G. Ashkenazi, R. Kosloff, S. Ruhman, and H. Tal-Ezer, J. Chem. Phys. **103**, 10005 (1995).
[46] G. R. Castro, D. Drakova, M. E. Grillo, and G. Doyen, J. Chem. Phys. **105**, 9640 (1996).
[47] G. R. Darling and S. Holloway, Rep. Prog. Phys. **58**, 1595 (1995).
[48] J. Harris, S. Holloway, T. S. Rahman, and K. Yang, J. Chem. Phys. **89**, 4427 (1988).
[49] M. R. Hand and S. Holloway, J. Chem. Phys. **91**, 7209 (1989).
[50] M. Persson, J. Strömquist, L. Bengtsson, B. Jackson, D. V. Shalashilin, and B. Hammer, J. Chem. Phys. **110**, 2240 (1999).
[51] T. N. Truong, D. G. Truhlar, and B. C. Garrett, J. Phys. Chem. **93**, 8227 (1989).
[52] C. Tully and G. D. Billing, Chem. Phys. Lett. **365**, 530 (2002).
[53] N. Geum, G.-H. Jeung, A. Derevianko, R. Cote, and A. Dalgarno, J. Chem. Phys. **115**, 5984 (2001).
[54] W. Kolos and L. Wolniewicz, J. Chem. Phys. **43**, 2340 (1965).
[55] R. Kosloff and H. Tal-Ezer, Chem. Phys. Lett. **127**, 223 (1986).
[56] R. Kosloff, Annu. Rev. Phys. Chem. **45**, 145 (1994).
[57] R. Kosloff, J. Phys. Chem. **92**, 2087 (1988).
[58] A. Vibok and G. G. Balint-Kurti, J. Chem. Phys. **96**, 7615 (1992).
[59] P. Brumer and M. Shapiro, Annu. Rev. Phys. Chem. **43**, 257 (1992).
[60] P. Brumer and M. Shapiro, Chem. Phys. Lett. **126**, 541 (1986).
[61] A. M. Weiner, J. P. Heritage, and E. M. Kirschner, J. Opt. Soc. Am. B **5**, 1563 (1988).
[62] K. A. Nelson, A. M. Weiner, D. E. Leaird, and G. P. Wiederrecht, J. Opt. Soc. Am. B **8**, 1264 (1991).
[63] A. D. Hammerich, J. G. Muga, and R. Kosloff, Isr. J. Chem. **29**, 461 (1989).